

Inelastic buckling of tapered members with accumulated strain

M.C. Kim[†] and G.C. Lee[‡]

Department of Civil Engineering, State University of New York at Buffalo, Buffalo, NY14260, U.S.A.

K.C. Chang[‡]

Department of Civil Engineering, National Taiwan University, Taipei, Taiwan

Abstract. This paper is concerned with inelastic load carrying capacity of tapered steel members with or without accumulated plastic strains resulted from previous loading histories. A finite element program is developed using stiffness matrices of tapered members and is applicable for analyses with material and geometric nonlinearity. Results of analyses are compared with other available solutions and with experimental results.

Key words: tapered member, inelastic buckling, accumulated strain

1. Introduction

Tapered members are frequently used for pin-based portal or gable frames in which maximum moments occur at eaves and decrease to approximately zero at the supports. Since Amirikian (1952) presented a simplified procedure for the analysis of such frames connected by hinges at the top center of the frames, extensive works have been done on tapered members both theoretically and experimentally (Bradford 1988, 1989, Bradford and Cuk 1988, Hwang, *et al.* 1991, Kitipornchai and Trahair 1972a, 1972b, Lee and Morrell 1974, 1975, Lee, *et al.* 1972, Lee and Szabo 1967, Prawel, *et al.* 1974, Salter, *et al.* 1980, Shiomi and Kurata 1983).

By varying the depth, almost uniform stress distribution along the member length can be achieved. Thus, the plastic zone could be more widely spread in a tapered member than a prismatic one under severe loadings. A shaking table test on a tapered gable frame model was conducted by Hwang, *et al.* (1991). The N-S component of 1940 EI Centro earthquake with different intensities were applied on the one fifth scale structural model. The frame, braced adequately in the lateral direction according to AISC specification, survived the largest intensity at first but failed by lateral buckling when the same loading was applied again. This is attributed to the accumulated strain resulted from previous loading cycles. From the strain measurement, it was found that about 75% of the rafter was in the inelastic range before failure. Predictions from various specifications showed considerable differences. All are conservative.

This paper is concerned with the capacity of tapered members with or without accumulated

[†] Formally Research Assistant

[‡] Professor

strains resulted from previous loading history. A finite element program is developed using stiffness matrices of tapered elements, applicable for large displacement problems. Strain hardening, residual stresses, and initial strains can all be taken into consideration. The stiffness matrices are derived from the total potential energy and then modified to account for large displacements. They are applied to linearly tapered elements for rectangular and I-sections. For illustrative purpose, elastic and inelastic buckling analyses are carried out on various tapered members and on a planar frame. The results are compared with other available solutions.

2. Finite element formulation

One dimensional finite element models for thin-walled prismatic members have been developed by many researchers since 1960s (Barsoum and Gallagher 1970, Bazant and Nimeiri 1973, Bradford 1988, 1989, Chan and Kitipornchai 1987, Rajasekaran and Murray 1973, Yang 1984). For tapered members, tapered elements is generally superior to uniform elements in convergence and accuracy. Stepped-member idealization of tapered member in most cases accompany slow convergence and inaccuracy because of imposed discontinuities and time-consuming data preparation. Shiomi (1983) and Salter (1980) had to use 30 uniform elements to represent a tapered member.

The one-dimensional finite element model for tapered members is derived from the energy theorem. To handle large displacement problems, stiffness matrices derived from the standard energy theorem using the displacement derivatives as generalized displacements are modified by adding the correction matrix to the rotational degrees of freedom locations in the geometric stiffness matrix (Argyris, *et al.* 1978, Elias 1986, Yang 1984). It is to be noted that the use of the conventional geometric stiffness matrix may lead to large errors when applied to a simple planar frame.

2.1. Stiffness matrices

Standard stiffness matrices for nonlinear analysis can be obtained either from the consideration of the total potential energy or from the virtual work. The total potential energy of a structural element is given by

$$\Pi = U - V \quad (1)$$

where U =the strain energy and V =the external work. For thin-walled members, U can be expressed as

$$U = \frac{1}{2} \int_v (\sigma_z \varepsilon_z + 2\tau_{zy} \varepsilon_{zy} + 2\tau_{zx} \varepsilon_{zx}) dv \quad (2)$$

in which the strain tensor can be separated into linear and nonlinear components as follows.

$$\varepsilon = \varepsilon_L + \varepsilon_{NL} \quad (3)$$

$$\begin{aligned} \varepsilon_z &= w_{,zz} + \frac{1}{2}(u_{,z}^2 + v_{,z}^2 + w_{,z}^2) \\ 2\varepsilon_{yz} &= v_{,z} + w_{,yz} + (u_{,y}u_{,z} + v_{,y}v_{,z} + w_{,y}w_{,z}) \end{aligned} \quad (4)$$

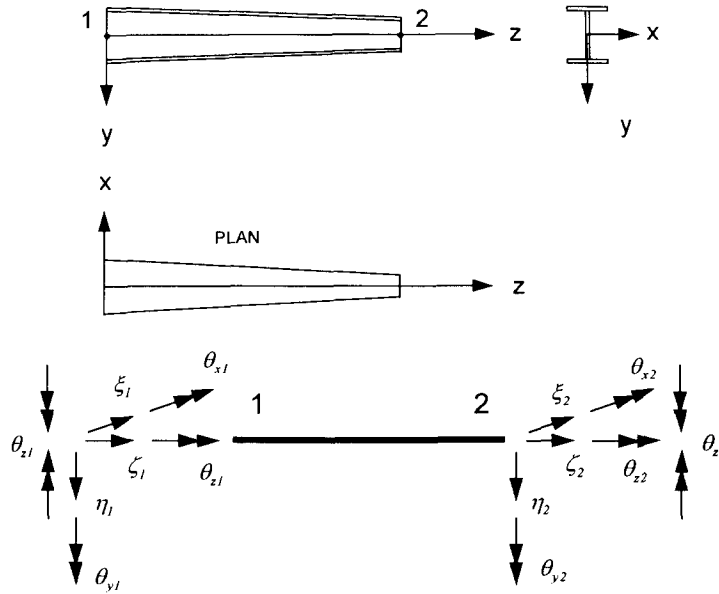


Fig. 1 Coordinate system and nodal degrees of freedom.

$$2\varepsilon_{xz} = u_{,z} + w_{,x} + (u_{,x}u_{,z} + v_{,x}v_{,z} + w_{,x}w_{,z})$$

In the first one of Eq. (4) the term $\frac{1}{2}w_{,z}^2$ may be neglected when compared to $w_{,z}$. Using the axis system shown in Fig. 1, the displacements may be written as

$$\begin{aligned} w &= \zeta - \xi'z - \eta'y - \theta'\omega \\ u &= \xi - (y - y_o)\theta \\ v &= \eta + (x - x_o)\theta \end{aligned} \quad (5)$$

The normal stress σ_z is

$$\sigma_z = \frac{P}{A} + \frac{M_x}{I_x}y - \frac{M_y}{I_y}x + \frac{B}{I_\omega}\omega \quad (6)$$

Neglecting higher order terms, the strain energy, U , can be obtained from Eq. (2) through Eq. (6).

Linear and cubic interpolation functions can be adopted for axial and other degrees of freedoms and the displacements in an elements are represented by their nodal values. Then the total potential energy can be expressed in a matrix form as

$$\Pi = \frac{1}{2}\tilde{\mathbf{r}}^T \bar{\mathbf{k}} \tilde{\mathbf{r}} - \tilde{\mathbf{F}}^T \tilde{\mathbf{r}} \quad (7)$$

$$\tilde{\mathbf{r}}^T = \{\xi_1, \xi_1, \eta_1, \theta_{z1}, \theta_{x1}, \theta_{y1}, \theta'_{z1}, \xi_2, \xi_2, \eta_2, \theta_{z2}, \theta_{x2}, \theta_{y2}, \theta'_{z2}\} \quad (8)$$

In the above equation, the subscripts 1 and 2 denote member ends. The stiffness coefficients are then obtained from

$$k_{ij} = k_{eij} + k_{gij} = \frac{\partial \Pi}{\partial r_i \partial r_j} \quad (9)$$

The above stiffness matrices obtained from the standard energy theorem may lead to large errors when applied to even a simple frame (Argyris, *et al.* 1978, Yang 1984). Thus, the geometric stiffness matrix k_g is modified by adding a three by three correction matrix, k_M , to the rotational degrees of freedom locations in the geometric stiffness matrix. It is referred to as k_{gs} . This transformation is necessary in order to ensure the continuity at the joints because the displacement derivatives in large displacement problems are generally not continuous at member ends where two or more members may be connected (Elias 1986). Yang and Argyris also obtained the above correction matrix by considering the nature of moments undergoing finite rotations in three dimensional space. Detailed expressions for the strain energy, stiffness matrices, and the correction matrix are given in Kim (1992).

2.2. Tapered elements

For tapered members, the linear stiffness matrix and a portion of the geometric stiffness should be reevaluated because the cross sectional dimensions are not constant along the member. For convenience in calculations the following properties are used. For I-sections,

$$\begin{aligned} A &= 2bt_f + t_w h \\ I_x &= \frac{t_w h^3}{12} + \frac{bt_f h^2}{2} \\ I_y &= \frac{t_f b^3}{6} + \frac{ht_w^3}{12} \\ I_w &= \frac{t_f h^2 b^3}{24} \\ J &= \frac{1}{3} ht_w^3 + \frac{2}{3} bt_f^3 \end{aligned} \quad (10)$$

All dimensions can be represented by their nodal values using linear interpolation. For rectangular sections one can simply substitute $b=0.0$. By substituting Eq. (10) into the potential energy expression and through Eqs. (7) and (9), the stiffness coefficients for tapered elements can be computed. All the integrations are carried out by using MACSYMA (1988).

2.3. Tangent stiffness coefficients

After portions of the cross section become yielded, the cross sectional properties must be reevaluated according to the assumed stress-strain idealization. Therefore, the strain energy should be modified and the equilibrium equations become incremental in nature. The transformed section is used to compute the tangent modulus of the cross section after yielding has initiated. For a given strain distribution, the transformed section is obtained by transforming the thickness of the plate segment of the cross section according to the ratio, E_s/E . Shear modulus, G does not influence the lateral buckling load much and it is therefore kept constant. The stress-strain relation, the typical transformed section, and the residual stress type adopted in this study are shown in Fig. 2 to Fig. 4.

Three types of residual stress are considered, Type A was used by Fukumoto and Galambos

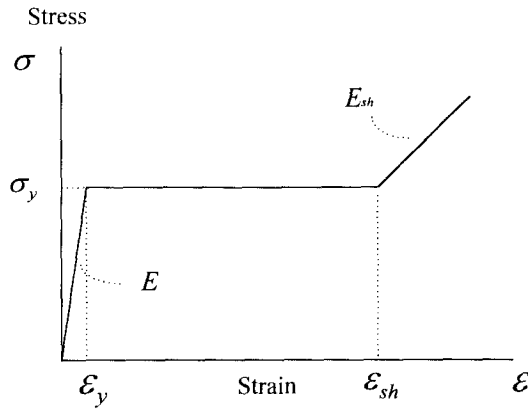


Fig. 2 Stress-strain idealization.

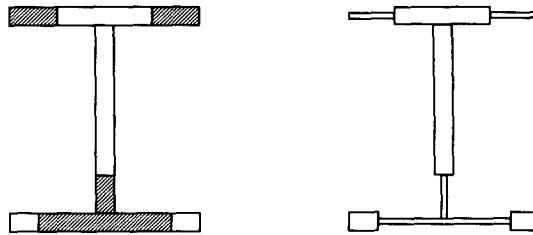


Fig. 3 Transformed I-section.

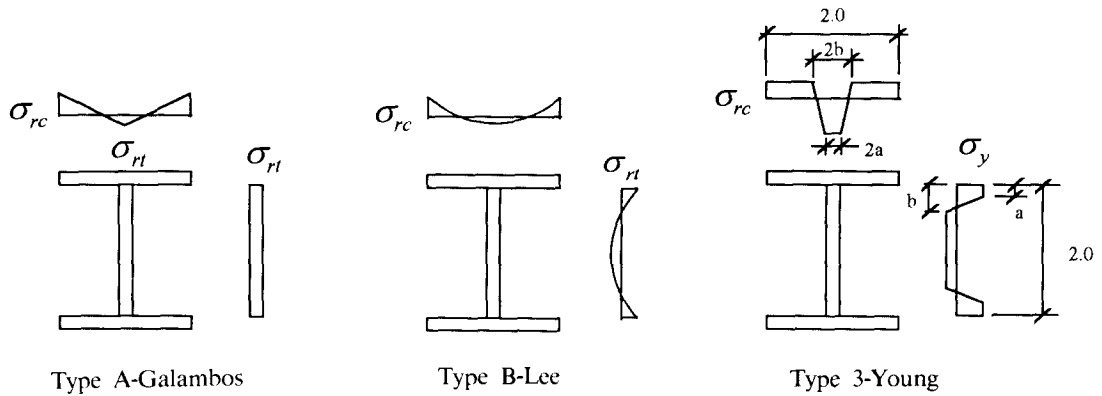


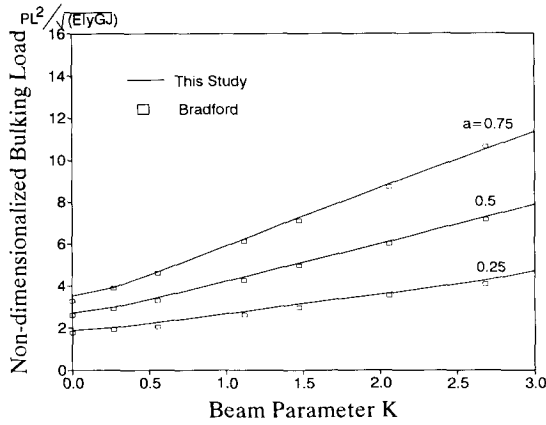
Fig. 4 Residual stress type.

(1966) Type B was used by Lee, and Type C was used by Young (1975). Type B satisfies the torsional equilibrium condition. The magnitude of the residual stresses in flanges and webs are given by

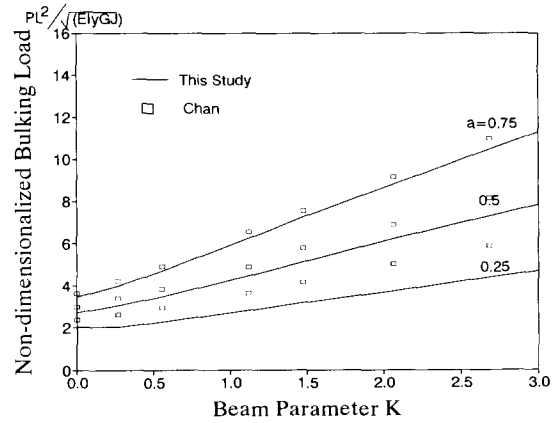
Type A:

$$\frac{\sigma_{rc}}{\sigma_y} = 0.3$$

$$\frac{\sigma_{rl}}{\sigma_y} = \frac{bt_f}{\{bt_f + t_w(h - t_f)\}} \quad (11)$$



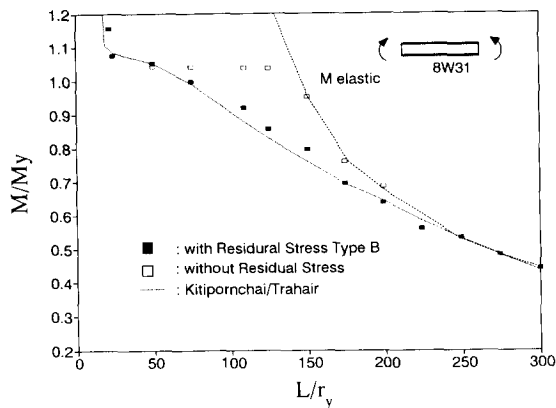
(a) Comparison with Bradford (1988);



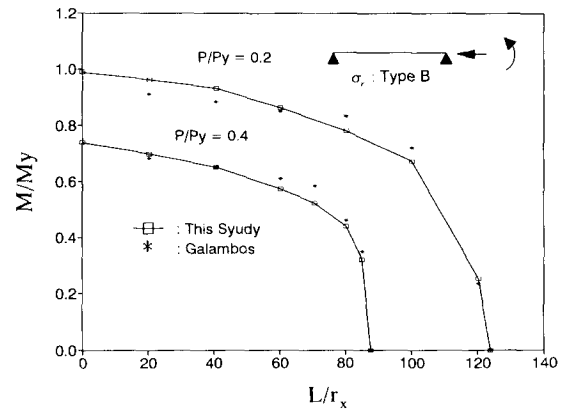
(a) Comparison with Chan (1990).

$$K = \frac{\pi}{L} \sqrt{\left(\frac{EI_w}{GJ} \right)},$$

Fig. 5 Flange tapered cantilever-centroidal loading.



(a) Equal and opposite moments at ends;



(b) Axial force and moment at one end.

Fig. 6 Inelastic buckling of a simply supported beam

Type B:

$$\begin{aligned} \sigma_{rf} &= c_1 x^4 + c_2 x^2 + \sigma_n \\ \sigma_{rw} &= c_3 y^4 + c_4 y^2 + \sigma_n \end{aligned} \quad (12)$$

Type C:

$$\frac{\sigma_n}{\sigma_y} = \frac{a+b}{2-(a+b)} \quad (13)$$

Typical values are -0.5, 0.3 for σ_n , σ_n respectively for rolled sections- type B and $a=0.08$, $b=0.29$

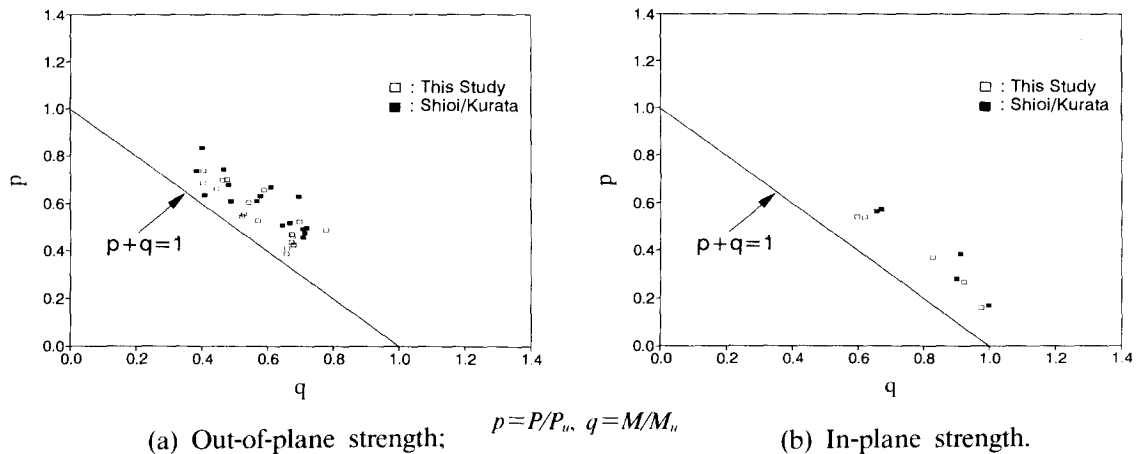


Fig. 7 Inelastic buckling of web tapered beam-columns

for type C.

2.4. Accumulated strain distribution

Strains accumulated during the previous loading history are assumed to be linear across the cross sections. Without knowing the previous load cycles, to predict the exact equilibrium paths is impossible. Therefore, the simple assumption is made that accumulated strains are added to each nodal points of the member. Only major axis strains are considered. The inelastic zone may be spread over large portion of the member under severe loadings. It is assumed that the accumulated strain at the larger end of the tapered member is equal to the yield strain and that it is linearly decreased to zero along the member. The measured strain distribution along the rafter of the gable frame from Hwang, *et al's* (1991) tests before the last loading is shown in Fig. 10a (linearly interpolated). The assumed strain distribution along a member length, for $a_p=0.5, 1.2$, is shown in Fig. 8, where a_p is an index indicating the inelastic zone of the member.

3. Solution procedure

The element stiffness matrices are transformed and assembled to the global stiffness matrices through the direct stiffness procedure. Linearized buckling load is computed from the bifurcation analysis, which assumes that the initial equilibrium state is undeformed but stressed. The condition to satisfy then is that the determinant of the coefficient matrix of the equilibrium equation be equal to zero, i.e.,

$$\det(K_e(\lambda) + K_g(\lambda)) = 0 \quad (14)$$

In elastic buckling cases, the above equation is a standard eigenvalue problem because the elastic stiffness matrix is independent of the loading and the geometric stiffness matrix is proportional to the loading. However, in plastic buckling problems, both matrices are nonlinearly dependent upon the applied loadings. Thus, an iterative procedure is needed to establish the Eq.

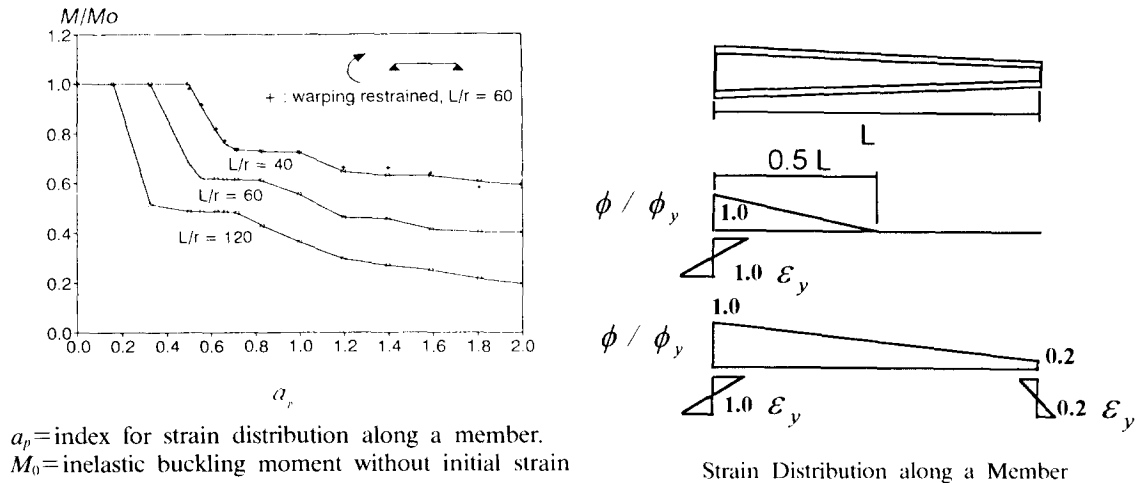


Fig. 8 Inelastic buckling of web tapered simple beam under a moment at one end.

- (14). The following scheme is adapted in this study. For a given load factor, λ
- (1) Solve the structure using elastic properties, calculate the member forces.
 - (2) Using displacements from the above, at each nodal points, compute the strain distributions including strains due to residual stress, accumulated strains, etc.
 - (3) Compute stress resultants for the above strain distributions using assumed models for the stress-strain relation.
 - (4) Calculate the unbalanced member forces.
 - (5) Adjust the strain distributions from the unbalanced forces.
 - (6) Repeat Step 3 to 5 until the value of the unbalanced forces are within the given tolerance.
 - (7) Construct the transformed section according to the current updated strain distributions.
 - (8) Compute the tangent stiffness matrices by assuming linear variations for the section properties.
 - (9) Solve the eigenvalue problem.

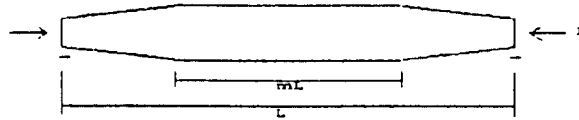
The lowest eigenvalue is searched by the secant method with the Sturm sequence check. Bisection and parabolic interpolation are used together to isolate the lowest eigenvalue.

4. Numerical examples

4.1. Elastic buckling

4.1.1. Tapered column

In Table 1, dimensionless critical loads of a hinged bar with tapered ends and with the prismatic central portion is evaluated for various taper ratios. The cross section is rectangular with $t_w=1.0$ mm, $h=10.0$ mm, and $E=71240$ Mpa. Due to symmetry, only half of the bar is modelled by using 6 elements. Results from this study agree well with available theoretical solutions (Timoshenko and Gere 1961).

Table 1 $[P_{cr}L^2/(EI_y)_l]$ 

Taper ratio γ	m									
	0		0.2		0.4		0.6		0.8	
	Pcr	Timo	Pcr	Timo	Pcr	Timo	Pcr	Timo	Pcr	Timo
0.1	6.49	6.48	7.60	7.58	8.69	8.63	9.48	9.46	9.82	9.82
0.2	7.01	7.01	8.00	7.99	8.92	8.91	9.56	9.63	9.83	9.82
0.4	7.87	7.87	8.61	8.59	9.25	9.19	9.67	9.70	9.85	9.84
0.6	8.60	8.61	9.10	9.12	9.50	9.55	9.75	9.76	9.86	9.85
0.8	9.26	9.27	9.51	9.54	9.70	9.69	9.82	9.83	9.86	9.86
1.0	9.87	9.87	9.87	9.87	9.87	9.87	9.87	9.87	9.87	9.87

4.1.2. Flange tapered cantilever beam

Elastic buckling load of a flange tapered cantilever beam which has the tapering ratio of 0.167 is investigated in this example. At the support (larger end), sectional dimensions are $b=12$ in., $h=24$ in., $t_w=0.375$ in., and $t_f=0.5$ in. The load is applied at the centroid of the tip of the cantilever and the critical load is non-dimensionalized by $P_{cr}L^2/(EI_y)_l$, where the subscript l denotes the larger end. The results from this study and those of Bradford's (1988) are in good agreement. They are shown in Fig. 5. However, Chan's (1990) predictions differ considerably when the taper ratio is small. Rapid decreases in the buckling loads are notable as the taper ratio decreases.

4.2. Inelastic buckling

4.2.1. Prismatic members

Inelastic buckling loads of a simply supported W8×31 section under equal and opposite moments at the ends are shown in Fig. 6a. The predictions of this study compares well with those of Trahair and Kitipornchai (1972b). Stiff increases near the yield moment are due to strain hardening. $\varepsilon_{sh}=11.0 \varepsilon_y$ and $E_{sh}=E/33.0$ are used in this example. Also shown in Fig. 6b are the inelastic lateral buckling strength under an axial load and a moment at one end of the same member. Again, the results are in good agreement with those of Fukumoto and Galambos (1966).

4.2.2. Tapered members

Inelastic buckling loads of web tapered I-sections are computed and compared with the results from the experiments conducted by Shiomi and Kurata (1983) – 19 tests for the lateral buckling and 5 tests for the in-plane strength. Comparisons are given in Fig. 7. Cross sectional dimensions are referred to Shiomi and Kurata (1983). Residual stress type C is used in this study. Solid line indicates the interaction equation for equivalent beams and columns. Despite the slight scatter, the finite element program of this study performs better than the interaction formula

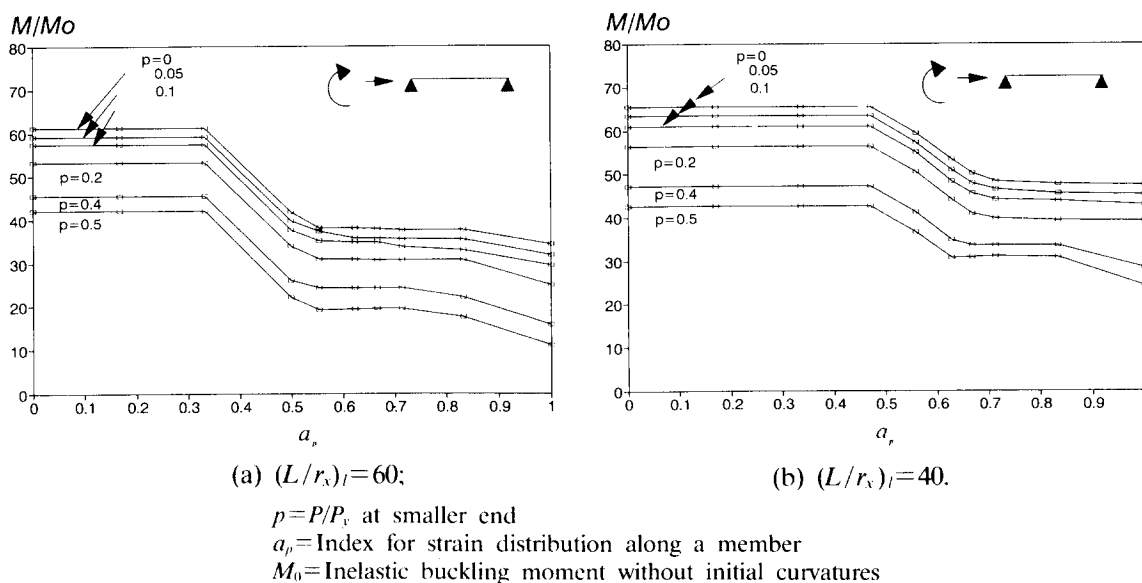


Fig. 9 Inelastic buckling of a web-tapered simple beam under moment and axial force

in predicting both the out-of-plane and the in-plane strength of the tapered beam-columns.

4.2.3. Tapered members with accumulated strain

Because of the lack of test data, strain distribution along a member due to previous loading cycles has to be assumed. It is therefore assumed that the yield strain is developed at larger end of the member (Fig. 8) as an initial strain condition. A simply supported tapered beam is considered in this example. Sectional dimensions are $b = 1.5$ in., $t_f = t_w = 0.125$ in., and $d = 5.625$, 1.75 in. for larger and smaller end respectively. The buckling moments are represented by dimensionless factor M/M_0 , where M_0 being the buckling moment without initial strains. Fig. 8 shows the degradation of the capacity of the tapered member as the accumulation of the strain increases. Warping restraint greatly enhance the resistance of the member as seen in the figure. Buckling moments of more slender members which fails elastically drop much faster than stocky ones. However, the ultimate strength is maintained for members with small slenderness ratio even though about half of the length of the member is left in inelastic range.

Inelastic buckling moments of the same member when a axial force is present are shown in Fig. 9a and Fig. 9b for the slenderness ratio of 40 and 60 respectively. When the axial forces are small, less than one tenth of P_y , there are only slight decreases in inelastic buckling moments if only small portions of the member are in the plastic zone. However, as the inelastic zone increases axial forces will reduce the resistance of the member. Both Fig. 8 and Fig. 9 show similar trends, i.e., ultimate strengths are retained until the inelastic zone reaches to a certain part of the member. Afterwards, the buckling curves drop to form plateaus and decrease slowly as the inelastic zone increases. This is expected because the moment decreases linearly from the larger end to zero at the smaller end so that the inelastic buckling is governed by the weakening of the larger end of the member.

Fig. 10a shows the assumed accumulated strain distributions along the rafter of the tapered gable frame during Hwang, *et al*'s test (1991) (linear variation between measured points is assumed).

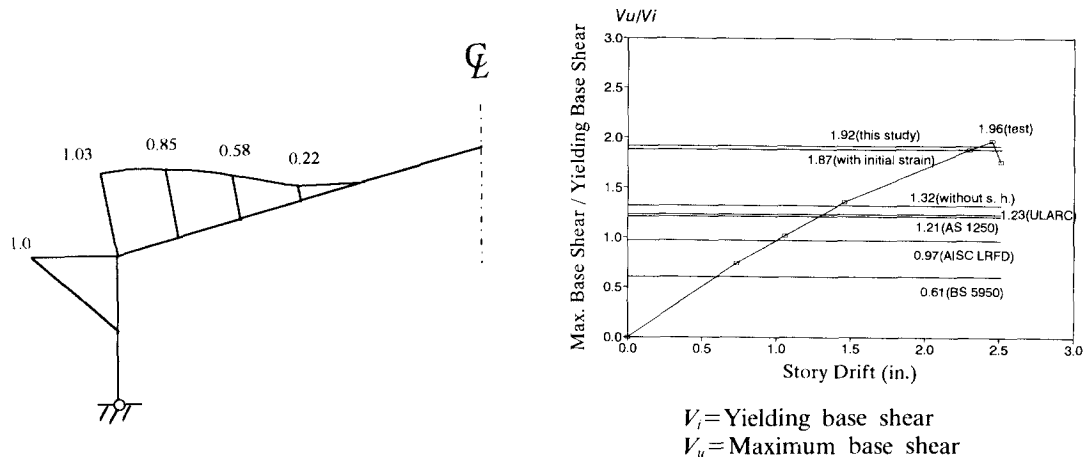


Fig. 10 (a) Strain distribution in the gable frame, ϵ/ϵ_y ; (b) Envelope curve of the tapered gable frame.

Applying these strain distributions, the predicted buckling loads are compared with the experimental results and other predictions by different codes in Fig. 10b. The finite element solution gives very close predictions to the ultimate strength of the frame. Also shown is the prediction when the strain hardening is neglected.

5. Concluding remarks

The effects of accumulated strain distributions along the tapered members due to previous loading cycles such as earthquake ground motions are investigated. The program predicts closely the elastic and inelastic buckling loads, with or without initial strains, of tapered and prismatic members.

It is found that adequate lateral bracings and warping restraints are important factors influencing the ultimate strength of tapered members. The ultimate strengths are maintained for stocky members even when the inelastic zone is spread over about half of the member.

The finite element program of this paper can be used for further studies which include the effect of the degradation of stiffness resulting from the previous cyclic loadings, other loadings and boundary conditions.

References

- Amirikian, A. (1952). "Wedge-beam framing", *Trans. ASCE*, **117**, 596.
- Argyris, J. H., Dunne, P. C., Malejannakis, G. A. and Scharpf, D. W. (1978), "On large displacement-small strain analysis of structures with rotational degrees of freedom", *Comput. Methods Appl. Mech. Eng.*, **14**, 401-451, **15**, 99-135.
- Argyris, J. H., Hilbert, O., Malejannakis, G. A. and Scharpf, D. W. (1979), "On the geometrical stiffness of a beam in space-a consistent v.w. approach", *Comput. Methods Appl. Mech. Eng.*, **20**, 105-131.
- Barsoum, R. S. and Gallagher, R. H. (1970). "Finite element analysis of torsional and torsional-flexural stability problems", *International J. for Num. Methods in Eng.*, **2**, 335-352.
- Bazant, Z. P. and Nimeiri, M. E. (1973), "Large-deflection spatial buckling of thin-walled beams and frames", *J. Struct. Eng.*, ASCE, **99**, 1259-1281.

- Bradford, M. A. (1988), "Stability of tapered I-beams", *J. Construct. Steel Res.*, **9**, 195-216.
- Bradford, M. A. (1989), "Inelastic buckling of tapered monosymmetric-I beams", *Eng. Struct.*, **11**, Apr., 119-126.
- Bradford, M. A. and Cuk, P. E. (1988), "Elastic buckling of tapered monosymmetric I-beams", *J. Struct. Eng.*, ASCE, **114**(ST5), 977-996.
- Chan, S. L. (1990), "Buckling analysis of structures composed of tapered members", *J. Struct. Eng.*, ASCE, **116**, Jul. 1893-1906.
- Chan, S. L. and Kitipornchai, S. (1987), "Geometric nonlinear analysis of asymmetric thin-walled beam-columns", *Eng. Struct.*, **9**, Oct. 243-254.
- Elias, Z. (1986), *Theory and methods of structural analysis*, John Wiley and Sons, Inc.
- Fukumoto, Y. and Galambos, T. V. (1966), "Inelastic lateral-torsional buckling of beam-columns", *J. Struct. Div.*, *Proc. ASCE*, **92**(ST2), Apr. 41-61.
- Hwang, J. S., Chang, K. C. and Lee, G. C. (1991), "Seismic behavior of gable frame consisting of tapered members", *J. Struct. Eng.*, ASCE, **117**, Mar. 808-821.
- Kim, M. C. (1992), "Elastic and inelastic buckling analysis of tapered members with accumulated strain", *Ph. D. Thesis*, SUNY at Buffalo.
- Kitipornchai, S. and Trahair, N. S. (1972a), "Elastic stability of tapered I-beams", *J. Struct. Div. Proc. ASCE*, **98**(ST3), 713-727.
- Kitipornchai, S. and Trahair, N. S. (1972b), "Buckling of inelastic I-beams under uniform moment", *J. Struct. Div.*, ASCE, **98**(ST11), 2551-2566.
- Lee, G. C. and Morrell, M. L. (1974), "Allowable stress for web-tapered beams with lateral restraints", *WRC Bul.*, **192**, Feb.
- Lee, G. C. and Morrell, M. L. (1975), "Application of AISC design provision for tapered members", *Eng. J.*, AISC, First Qtr., 1-13.
- Lee, G. C., Morrell, M. L. and Ketter, R. L. (1972), "Design of tapered members", *WRC Bul.* **173**.
- Lee, G. C. and Szabo, B. A. (1967), "Torsional response of tapered I-girders", *J. Struct. Div.*, ASCE, **93**, Oct., 233-252.
- Prawel, S. P., Morell, M. L. and Lee, G. C. (1974), "Bending and Buckling strength of tapered structural members", *Welding Res. Suppl.*, Feb., 75-s.
- Rajasekaran, S. and Murray, D. W. (1973), "Finite element solution of inelastic beam equations", *J. Struct. Div.*, ASCE, **99**(ST6), 1025-1041.
- Salter, J. B., Anderson, D. and May, I. M. (1980), "Tests on tapered steel column", *The Structural Engineer*, **58**(6), 189-193.
- Shiomi, H. and Kurata, M. (1983), "Strength formula for tapered beam-columns", *J. Struct. Eng.*, ASCE, **110**(7), 1630-1643.
- Timoshenko, S. P. and Gere, J. M. (1961), *Theory of elastic stability*, McGraw-Hill, New York.
- Vlasov, V. Z. (1961), *Thin walled elastic beams*, NSF, 2nd ed.
- Yang, Y. B. (1984), "Linear and nonlinear analysis of space frames with nonuniform torsion using interactive computer graphics", *Ph. D. Thesis*, Cornell U., Ithaca, Y.
- Young, B. W. and Robinson, K. W. (1975), "Buckling of axially loaded welded steel columns", *The Structural Engineer*, **53**(5), May, 203-207.
- MACSYMA Group (1988), *The MACSYMA reference manual*, Symbolics, Inc., Eleven Cambridge Center, Cambridge, MA 02142.